8768 *Biochemistry* **2009,** *48,* 8768–8770
DOI: 10.1021/bi9012726

BIOCHEMISTRY
including biophysical chemistry & molecular biology
Rapid Report

Structure of Psb27 in Solution: Implications for Transient Binding to Photosystem II during Biogenesis and Repair[†,‡,§]

Kai U. Cormann,[⊥] Jan-Amadé Bangert,[∥] Masahiko Ikeuchi,[∥] Matthias Rögner,[⊥] Raphael Stoll,*[,∥] and Marc M. Nowaczyk*[,⊥]

[⊥]*Department of Plant Biochemistry and Biomolecular NMR, Ruhr-University Bochum, D-44780 Bochum, Germany, and* [∥]*Department of Life Sciences (Biology), University of Tokyo, 3-8-1 Komaba, Meguro-ku, Tokyo 153-8902, Japan*

Received July 24, 2009; Revised Manuscript Received August 21, 2009

ABSTRACT: Psb27 is a membrane-extrinsic subunit of photosystem II (PSII) where it is involved in the assembly and maintenance of this large membrane protein complex that catalyzes one of the key reactions in the biosphere, the light-induced oxidation of water. Here, we report for the first time the structure of Psb27 that was not observed in the previous crystal structures of PSII due to its transient binding mode. The Psb27 structure shows that the core of the protein is a right-handed four-helix bundle with an up−down−up−down topology. The electrostatic potential of the surface generated by the amphipathic helices shows a dipolar distribution which fits perfectly to the major PsbO binding site on the PSII complex. Moreover, the presented docking model could explain the function of Psb27, which prevents the binding of PsbO to facilitate the assembly of the Mn_4Ca cluster.

Photosystem II (PSII) is a large multisubunit membrane protein complex located in the thylakoid membranes of cyanobacteria, algae, and vascular plants. It catalyzes one of the most important reactions in nature, the light-induced oxidation of water. Oxygen is released as a byproduct in this reaction, leading to an aerobic atmosphere which was the prerequisite for the development of all animal life on our planet. This water-splitting reaction is catalyzed by a Mn_4Ca cluster which is surrounded by at least three extrinsic proteins on the luminal side of the complex. These proteins, especially the PsbO subunit, play an important role in the stabilization and optimization of the oxygen evolving activity (for a review, see ref *1*). Several crystal structures of PSII complexes from thermophilic cyanobacteria (*2*, *3*) shed light on the structural organization of this enigmatic complex. In the most recent model (*4*), 20 subunits, 35 chlorophyll *a* molecules, 12 carotinoids, three quinones, two pheophytins, and 25 integral lipids as well as several inorganic cofactors (Mn^{n+}, Ca^{2+}, Cl^-, and $Fe^{2+/3+}$) have been traced.

Precise positioning of the redox active cofactors and the surrounding proteins is pivotal for the proper function of the complex. Therefore, the assembly of proteins and cofactors has to occur in a highly coordinated manner (for a review, see ref *5*). Moreover, the use of light and the presence of oxygen inherently lead to constant damage of the PSII complex. To prevent persistent inactivation, the damaged proteins, mainly the D1 core subunit, are continuously replaced in a unique mechanism, called the PSII repair cycle (for a review, see ref *6*). During this cycle, the PSII complex is partly disassembled, the damaged D1 core subunit is exchanged, and the complex is activated again. In particular, incorporation of manganese and formation of the oxygen-evolving complex are crucial steps during this process and require critical control. Hence, incorporation of manganese occurs only after C-terminal processing of D1, catalyzed by the CtpA protease (*7*) which is guided by the TPR protein PratA (*8*). After D1 processing, a transient PSII−Psb27 complex is formed (*9*, *10*) which prevents binding of the extrinsic subunits (*9*) to facilitate incorporation of manganese (*11*). In cyanobacteria, the Psb27 subunit (*12*, *13*) exhibits a specific lipid modification that seems to be involved in binding to the complex (*9*). After or during incorporation of manganese, the Psb27 subunit is released and the extrinsic proteins bind to the luminal side of PSII to generate the active complex. Although Psb27 plays an important role in the assembly of PSII in cyanobacteria (*9*, *11*, *14*) and plants (*15*), to date the structural details of the Psb27 protein or of the transient PSII−Psb27 complex are still completely unknown. Here we report for the first time the three-dimensional structure in solution of Psb27 from the cyanobacterium *Synechocystis* PCC 6803 and discuss its functional implications during biogenesis and repair of PSII.

The structure of Psb27 was determined by heteronuclear multidimensional NMR data using uniformly ^{15}N-labeled and ^{13}C- and ^{15}N-labeled samples. Twenty final structures of 100 were selected on the basis of their lack of restraint violations, energetic favorability, and deviations from ideal bond lengths and angles (Table S1 of the Supporting Information). For this family (Figure 1A), experimental restraints were well-satisfied with no nuclear Overhauser effect (NOE) violation exceeding 0.5 Å and no difference in torsion angle of $> 5.0°$. After refinement, the structures show a root-mean-square deviation (rmsd) of 1.74 Å for the backbone atoms of the entire protein and 0.81 Å for the backbone in the helical regions (Table S1). The model with the overall lowest-energy term was selected as the representative structure (Figure 1B).

The structure of the Psb27 protein consists of a short flexible linker domain (residues 1−6) which is usually attached to the membrane by an N-terminal lipid anchor (*9*) and a well-folded domain that extends from residue 7 to the carboxy terminus. The folded domain has a right-handed four-helix bundle structure

[†]This work was supported by grants (SFB480 to M.R. and SFB642 to R.S.) from the DFG, SolarH2 and the Protein Research Department of the Ruhr-University Bochum.
[‡]Coordinates have been deposited under accession code 2KND in the PDB databse.
[§]This paper is dedicated to Prof. Dr. Achim Trebst on the occasion of his 80th birthday.
*To whom correspondence should be addressed. R.S. (for the NMR part): phone, 49-234-32-25466; fax, 49-234-32-05466; e-mail, raphael.stoll@rub.de. M.M.N.: phone, 49-234-32-23657; fax, 49-234-32-14322; e-mail, marc.m.nowaczyk@rub.de.

 Published on Web 08/21/2009

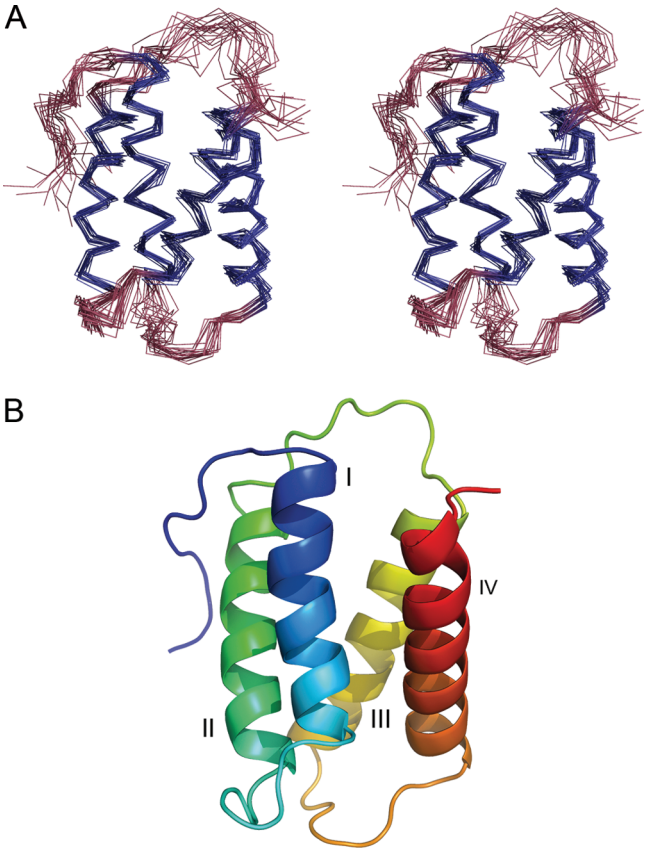

FIGURE 1: (A) Stereoview of the backbone atoms of 20 Psb27 structures. Helical regions are colored blue, whereas the termini and loop regions are colored dark red. (B) The structure with the lowest-energy term illustrates the fold of a right-handed four-helix bundle with an up−down−up−down topology.

with dimensions of approximately 35 Å × 22 Å × 16 Å. The four α-helices (I−IV) that span residues 11−27, 36−51, 64−79, and 89−107 are connected by short turns to form a bundle with an up−down−up−down topology (Figure 1). The superposition of the final structures clearly shows that the backbone is well-defined in the helical regions as well as in two loop regions comprising residues 28−35 (α1−α2 loop) and 80−88 (α3−α4 loop). The segments between residues 1−7 (N-terminus) and 53−62 (α2−α3 loop) show the lowest precision of atomic coordinates in the NMR ensemble of structures. The core structure is stabilized by hydrophobic interactions of the four amphipathic helices, and interestingly, the N-terminal region is obviously attached to helix II by close contacts between L7 and Y49. The three-dimensional arrangement of the four amphipatic helices of Psb27 generates an electrostatic surface that is differently charged on opposite sides (Figure 2). An acidic surface is formed by aspartate and glutamate residues located in helices I, II, and IV, whereas positively charged amino acids occur on the backside of helix IV as well as in the loop regions connecting helices II, III, and IV. Notably, helix III is surrounded by basic residues. However, the surface of the helix itself is uncharged (Figure 2C). With the exception of F99, all aromatic residues lie at the beginning or at the end of a helix so that the side chains are at least partially exposed to the solvent.

The steady-state heteronuclear $^{15}N\{^1H\}$ NOE for the backbone amides of Psb27 (Figure S1) indicates that most of the 110 residues of Psb27 are part of a compact fold as these residues exhibit values of ~0.8. Missing data points originate from proline

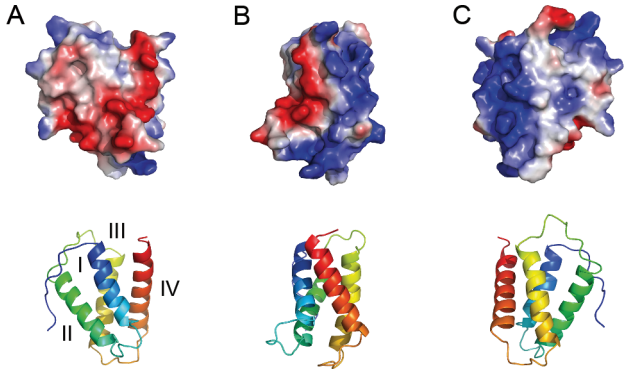

FIGURE 2: Electrostatic surface potential of Psb27. A negatively charged surface (colored red) is formed by helices I, II, and IV (A). Notably, helix IV contains a number of basic residues on the backside of the anionic surface (B). The positively charged surface (colored blue) is formed by helix IV and the loop regions between helices II, III, and IV that surround the uncharged surface of helix III (C).

residues, C1, and from resonances that exhibited a high degree of overlap in the NMR spectra; therefore, data could not be extracted. The N-terminus as well as the αI−αII and αIII−αIV loops partially exhibit slightly lower values for the $^{15}N\{^1H\}$ NOE which is reflected in the NMR ensemble by elevated root-mean-square deviation (rmsd) values (Figures 1 and S1). The αII−αIII loop that is comprised of residues S51−L62 exhibits $^{15}N\{^1H\}$ NOE values around or even below 0.6. This clearly suggests an increased flexibility for this αII−αIII loop on the pico- to nanosecond time scale, in concordance with only a limited number of NOEs that could be extracted for this loop from the spectra. Thus, the αII−αIII loop is ill-defined in the solution state because of genuine fluctuations rather than a lack of experimental restraints (Figures 1 and S1). At the C-terminus, the last five residues show slightly decreased values for the $^{15}N\{^1H\}$ NOE (Figure S1). The assembly of the water splitting machinery takes place at the luminal side of PSII guided by the Psb27 protein. It was shown previously that binding of Psb27 blocks the association of the other extrinsic proteins (*9*), presumably by preventing the attachment of PsbO. To screen for potential docking sides of Psb27 that fit on the basis of shape and electrostatics, we modeled the luminal surface of *Synechocystis* PSII (for details, see the methods section). One of the most feasible solutions calculated without any experimental constraints is shown in Figure 3. Psb27 might interact with PSII by binding of helices III and IV to an oppositely charged binding niche mainly formed by the CP47 subunit (Figure 3A). This part of the luminal surface represents the main binding site for PsbO in the active complex (Figure 3B) which would explain the antagonistic function of Psb27.

Interestingly, the PsbO loop responsible for binding shows a charge distribution on its surface similar to that of Psb27 (Figure 2), thus matching the inverted electrostatic surface potential of the PSII binding site. The same pattern is found in *Thermosynechococcus elongatus* (data not shown). Moreover, three amino acids at the suggested docking site of Psb27 that are important for the dipolar charge of helix IV (R94, E103, and R107) are highly conserved among cyanobacteria (Figure S2).

In our model, the N-terminus of Psb27 is located toward the monomer−membrane interface of the monomeric complex (Figure 3). As native Psb27 exhibits an N-terminal lipid modification (*9*) that should be located in a hydrophobic environment, this location may explain the open question of how Psb27 is released from monomeric PSII during biogenesis: while a strong

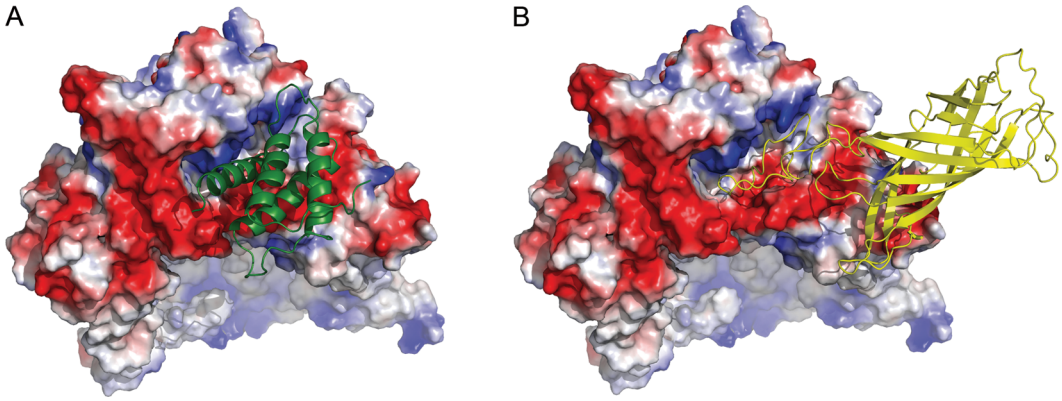

FIGURE 3: Docking model of Psb27 and the PSII complex. The electrostatic surface potentials calculated with PyMol (*16*) are shown for the luminal surfaces of PsbA, PsbB, and PsbD which were modeled for *Synechocystis* on the basis of the PSII structure of Ferreira et al. (*2*). The potential location of Psb27 (A, colored green) and the binding site of PsbO (B, colored yellow) are indicated. Acidic residues are colored red and basic residues blue, and the membrane intrinsic part is shaded in gray.

hydrophobic interaction between Psb27 and PSII solubilized in detergent micelles was described previously (*9*), the release of this interaction might be much easier in the native lipid environment of the thylakoid membrane. A prerequisite is that the lipid anchor of Psb27 be located in the lipid phase next to the monomer−membrane interphase as suggested by our model and not in the hydrophobic core of the complex. This would enable a quick release of Psb27 from preassembled PSII complexes followed by the assembly of the extrinsic proteins without the need for a specific lipase or other cofactors.

ACKNOWLEDGMENT

We thank G. Kock for stimulating discussions, and we are grateful to Prof. Dr. von Kiedrowski for providing access to the DRX600 spectrometer.

SUPPORTING INFORMATION AVAILABLE

Detailed methodology, NMR statistics, heteronuclear NOE results, and a multiple-sequence alignment. This material is available free of charge via the Internet at http://pubs.acs.org.

REFERENCES

1. Roose, J. L., Wegener, K. M., and Pakrasi, H. B. (2007) *Photosynth. Res. 92*, 369–387.
2. Ferreira, K. N., Iverson, T. M., Maghlaoui, K., Barber, J., and Iwata, S. (2004) *Science 303*, 1831–1838.
3. Kamiya, N., and Shen, J. R. (2003) *Proc. Natl. Acad. Sci. U.S.A. 100*, 98–103.
4. Guskov, A., Kern, J., Gabdulkhakov, A., Broser, M., Zouni, A., and Saenger, W. (2009) *Nat. Struct. Mol. Biol. 16*, 334–342.
5. Nickelsen, J., Nowaczyk, M. M., and Klinkert, B. (2007) in Progress in Botany (Esser, K., Lüttge, U. E., Beyschlag, W., and Murata, J., Eds.) pp 57−79, Springer-Verlag, Berlin.
6. Mulo, P., Sirpio, S., Suorsa, M., and Aro, E. M. (2008) *Photosynth. Res. 98*, 489–501.
7. Anbudurai, P. R., Mor, T. S., Ohad, I., Shestakov, S. V., and Pakrasi, H. B. (1994) *Proc. Natl. Acad. Sci. U.S.A. 91*, 8082–8086.
8. Klinkert, B., Ossenbuhl, F., Sikorski, M., Berry, S., Eichacker, L., and Nickelsen, J. (2004) *J. Biol. Chem. 279*, 44639–44644.
9. Nowaczyk, M. M., Hebeler, R., Schlodder, E., Meyer, H. E., Warscheid, B., and Rogner, M. (2006) *Plant Cell 18*, 3121–3131.
10. Mamedov, F., Nowaczyk, M. M., Thapper, A., Rogner, M., and Styring, S. (2007) *Biochemistry 46*, 5542–5551.
11. Roose, J. L., and Pakrasi, H. B. (2008) *J. Biol. Chem. 283*, 4044–4050.
12. Ikeuchi, M., Inoue, Y., and Vermaas, W. (1995) in Photosynthesis: From Light to Biosphere (Mathis, P., Ed.) pp 297−300, Kluwer Academic Publishers, Dordrecht, The Netherlands.
13. Kashino, Y., Lauber, W. M., Carroll, J. A., Wang, Q., Whitmarsh, J., Satoh, K., and Pakrasi, H. B. (2002) *Biochemistry 41*, 8004–8012.
14. Bentley, F. K., Luo, H., Dilbeck, P., Burnap, R. L., and Eaton-Rye, J. J. (2008) *Biochemistry 47*, 11637–11646.
15. Chen, H., Zhang, D., Guo, J., Wu, H., Jin, M., Lu, Q., Lu, C., and Zhang, L. (2006) *Plant Mol. Biol. 61*, 567–575.
16. DeLano, W. L. (2002) The PyMol Molecular Graphics System, DeLano Scientific, Palo Alto, CA.